RSC Advances

PAPER

View Article Online
View Journal | View Issue

Cite this: *RSC Adv.*, 2017, **7**, 1966

Preparation of mesoporous $SiO_2/Bi_2O_3/TiO_2$ superhydrophilic thin films and their surface self-cleaning properties†

Zhaogao Bai,[a] Yun Hu,*[abc] Shuqin Yan,[a] Wenjie Shan[a] and Chaohai Wei[ab]

Received 31st October 2016
Accepted 21st December 2016

DOI: 10.1039/c6ra26078k

www.rsc.org/advances

Mesoporous $SiO_2/Bi_2O_3/TiO_2$ triple-layered thin films were prepared on glass slides using a simple sol–gel/spin-coating method. For comparison, double-layered Bi_2O_3/TiO_2 and mixed Bi_2O_3–TiO_2 thin films were prepared using the same method. The obtained samples were characterized by X-ray diffraction (XRD), UV-vis spectrophotometry (UV-vis), scanning electron microscopy (SEM), X-ray photoelectron spectroscopy (XPS) and contact angle measurements. Methyl orange was used as a model pollutant to evaluate the photocatalytic properties of the thin films. The self-cleaning properties of the thin films were investigated by tracking the photocatalytic removal of stearic acid. The mesoporous $SiO_2/Bi_2O_3/TiO_2$ multi-layered thin films retained the mesoporous structure of SiO_2, demonstrating superhydrophilicity and antifogging ability even in the dark, as well as more efficient photocatalytic behavior than double-layered Bi_2O_3/TiO_2 and mixed Bi_2O_3–TiO_2 thin films when illuminated with weak UV light irradiation. Moreover, the thin films resisted both acidic and alkali corrosion of the type they might encounter in the natural environment.

1. Introduction

Titanium dioxide (TiO_2) is one of the best candidates for use in photovoltaic and photocatalytic devices due to its chemical stability, low cost, and non-toxicity.[1] Ever since Wang first reported the superhydrophilicity (contact angle below 5°) of TiO_2 thin films, light-induced superhydrophilicity of solid surfaces has attracted considerable interest.[2] These films on glass slides have additional properties that make them attractive for use in solar cells (*i.e.*, they are self-cleaning and antifogging) and in decontamination applications.[3–5] A pure titanium film can only be activated under UV light, and photo-induced carriers are easily eliminated by recombination which severely limits the widespread application of such films.[6] Many efforts have been made to overcome this problem. For example, TiO_2 has been modified by various strategies, such as coupling with a narrow band gap semiconductor,[7–9] doping with a metal or non-metal ion,[10–12] co-doping with two or more foreign ions,[13–16] surface sensitization by organic dyes or metal complexes,[17–19] surface fluorination[20,21] and noble metal deposition.[22] These modifications have resulted in higher quantum efficiencies and increased rates of the degradation of organic pollutants under UV or solar light.

Semiconductor coupling is a particularly promising way of improving the photocatalytic efficiency of TiO_2. Coupling TiO_2 with a metal sulfide (*e.g.*, PbS/TiO_2 (ref. 23) and CdS/TiO_2 (ref. 24 and 25)) or with a metal oxide semiconductor (*e.g.*, Cu_2O/TiO_2,[26] WO_3/TiO_2 (ref. 27) and ZnO/TiO_2 (ref. 28)) has received significant attention in recent years. The photocatalytic activity of these coupled semiconductors is higher than that of the single semiconductor alone. This behavior has been ascribed to the semiconductor–semiconductor heterojunction system, which is beneficial to maintaining charge separation and reducing the limiting phenomenon of recombination.

Bi_2O_3 is a metal–oxide semiconductor with a narrow band gap, more oxygen vacancies and strong oxidizing properties. It is one of the most promising new catalysts.[29] Wang *et al.* fabricated a TiO_2 film which was modified with Bi_2O_3 in a microgrid array using a microsphere lithography method.[30] The coupled system showed higher photocatalytic activity under xenon lamp irradiation than pure TiO_2 or Bi_2O_3 films alone. The enhancement of photocatalytic activity was ascribed to the special structure, which improved the separation of photo-generated electrons and holes. Xu *et al.* prepared the Bi_2O_3–TiO_2 composite films by a modified sol–gel method, and the film with Bi/Ti ratio of 1.25% showed higher surface hydroxyl group density and higher photocatalytic activity than pure TiO_2 under solar irradiation.[31] But the photocatalytic activity of the Bi_2O_3–TiO_2 composite films decreased if the Bi_2O_3 exceeded the optimum percentage because at those

[a]School of Environment and Energy, South China University of Technology, Guangzhou 510006, P. R. China. E-mail: huyun@scut.edu.cn; Tel: +86-20-39380573

[b]Guangdong Provincial Engineering and Technology Research Center for Environmental Risk Prevention and Emergency Disposal, Guangzhou 510006, P. R. China

[c]Guangdong Provincial Key Laboratory of Atmospheric Environment and Pollution Control, Guangzhou 510006, P. R. China

† Electronic supplementary information (ESI) available. See DOI: 10.1039/c6ra26078k

higher levels Bi_2O_3 becomes a recombination site of the charge carriers. However, this problem is not observed in Bi_2O_3/TiO_2 double-layered thin films, due to the different interface locations of Bi_2O_3 and TiO_2 in such films.

Surfaces possess wetting characteristics, such as superhydrophilicity or superhydrophobicity, which play an important role in many practical applications of these materials. These phenomena have already been applied to some self-cleaning products, such as window glasses, automotive glasses, tiles, mirrors and plastics. Zhang *et al.* reported that superhydrophilicity plays a significant role in the self-cleaning process.[32] As a result, more researchers have been exploring this phenomenon in recent years. In our previous study, we synthesized mesoporous SiO_2 thin films which exhibit superhydrophilicity under dark condition.[33] Thus, in order to enhance the self-cleaning property of the thin films, we synthesized mesoporous $SiO_2/Bi_2O_3/TiO_2$ triple-layered thin films *via* a simple sol–gel/spin-coating method. The mesoporous structure of the thin films and their optical, superhydrophilic and photocatalytic properties were investigated. Also, stearic acid and methyl orange were used as the models to investigate the decontamination and self-cleaning properties of the thin films.

2. Experimental section

2.1. Materials

Tetraethyl orthosilicate (TEOS, AR) and tetrabutyl titanate (TBOT, AR) were purchased from Tianjin Fu Chen chemical reagent factory. Bismuth nitrate pentahydrate ($Bi(NO_3)_3\cdot 5H_2O$, AR) was bought from Sinopharm chemical reagent company. Acetyl acetone (AA, AR) was supplied by Tianjin chemical reagent factory. $C_{12}H_{25}(OCH_2CH_2)_4OH$ (Brij^{R}30, AR) and Triton™ X-100 (OP, AR) were obtained from Sigma-Aldrich. Polyethylene glycol 200 (PEG 200, AR) and acetone (Ac, AR) were bought from Guangzhou chemical reagent factory. All reagents were analytical grade and used without further purification.

2.2. Preparation of layered thin films

Bi_2O_3/TiO_2 double-layered thin films. Commercial glass plates were used as substrates after being washed with ethanol, sodium hydroxide solution (10 wt%) and distilled water, followed dried at 100 °C for 3 h. The Bi_2O_3/TiO_2 double-layered thin films were synthesized by the sol–gel/spin coating method. The bottom-layer TiO_2 films were synthesized by sol–gel using TBOT as the titanium source. Briefly, 17 g of TBOT was added to 50 mL of ethanol and stirred for 30 min at 30 °C, after which 3.7 mL of acetyl acetone was added. The solution was labeled as A. At the same time, 0.045 mL of nitric acid, 3.6 mL of distilled water and 27.5 mL of ethanol were mixed and labeled as B. Then, B was added dropwise into A with vigorous stirring for 2 h, resulting in the formation of a transparent sol of TiO_2, which was then aged for 24 h. The molar ratio of above materials was: TBOT : EtOH : AA : HNO_3 : H_2O = 1 : 26.5 : 1 : 0.02 : 4. The sol was dropped onto a glass substrate which was spinning at a rate of 4000 rpm for 1 min, and then calcined to 550 °C for 5 h with a heating rate of 1 °C min^{-1}.

Thin Bi_2O_3 films were prepared with the sol–gel method.[34] 5 g of $Bi(NO_3)_3\cdot 5H_2O$ was dissolved in 4.2 mL of the nitric acid solution B. 2 mL of PEG 200, 2 g of citric acid and 10 mL of acetone were then added while 4 mL of OP was added as a surfactant. The solution was stirring for 3 h, as a sol solution formed. The Bi_2O_3/TiO_2 double-layer thin films were produced by spin-coating the Bi_2O_3 sol on top of the bottom-layer TiO_2 films. The spin-coating step was repeated until the desired coating times were obtained. Therefore the resulting Bi_2O_3/TiO_2 thin films were denoted as B(n)/T(n), n = 1, 3, 6, where n is coating times. All the thin films were calcined to 550 °C for 3 h at a heating rate of 1 °C min^{-1}. For comparison, TiO_2/Bi_2O_3 thin films denoted as T/B were produced by spin-coating the TiO_2 sol on top of the bottom-layer Bi_2O_3.

Three different mixed thin films consisting of Bi_2O_3 and TiO_2 were also prepared using varying proportions of the two materials. The resulting Bi_2O_3–TiO_2 mixed thin films were denoted as x% B–T, where x = 1, 3, 5.

Mesoporous $SiO_2/Bi_2O_3/TiO_2$ triple-layered thin films. SiO_2 sol was synthesized as reported previously.[33] TEOS, EtOH and Brij^{R}30 were used as precursor, solvent and surfactant, respectively. 10.4 g of TEOS and 18.25 mL of EtOH were mixed, after which 3.55 g of Brij^{R}30 and 0.155 mL of HCl were dropwise added into the solution, respectively. A clear solution with the molar ratio of TEOS : EtOH : Brij^{R}30 : HCl = 8.0 : 50 : 0.9 : 0.8 was obtained after stirring for 10 min at 30 °C. The SiO_2 sol was spin-coated on top of the Bi_2O_3/TiO_2 double-layered thin films. The resulting thin films were dried at 30 °C for 2 h and then calcined to 450 °C for 5 h at a heating rate of 1 °C min^{-1}. The resulting $SiO_2/Bi_2O_3/TiO_2$ triple-layered thin films were labeled as S/B/T.

2.3. Characterizations

The structures of the thin films were studied by X-ray diffraction (Bruker, D8) using Cu Kα (λ = 0.15406 nm). Optical transmission measurements were performed on a UV-vis spectrophotometer (Shimadzu, UV-2550). The binding energy was determined by X-ray photoelectron spectroscopy (XPS) with Mg Kα radiation (Axis Ultra DLD). The XPS peaks were calibrated with the C 1s peaks derived from a surface-contaminating hydrocarbon that had a binding energy of 284.4 eV. The morphologies of the films were characterized with scanning electron microscopy (SEM, Hitachi S-4800, FE-SEM) and high-resolution transmission electron microscope (HR-TEM, JEOL JEM-2100F). Water contact angles were obtained at room temperature using a commercial contact angle meter (Dataphysics OCA 15 plus) which has an accuracy of ±1°. A droplet of water was placed on the surface of the layered glass slide with a 1 μl micro-injector. Fourier transform infrared (FT-IR) spectra were obtained using a Thermo Nicolet 6700 with KBr disks containing the prepared samples.

2.4. Photocatalytic activity and self-cleaning measurements

Stearic acid and methyl orange were used as models to evaluate the self-cleaning properties and photocatalytic activity of the prepared samples. A methyl alcohol solution of stearic acid (1.5×10^{-3} mol L^{-1}) was dropped onto the samples and dried at 80 °C for 2 h. The photocatalytic degradation of methyl orange

was carried out in a vessel in which two samples (the total area is 12.5 cm^2) were placed in 100 mL of a 20 mg L^{-1} solution of methyl orange. A 125 W high pressure mercury lamp with an intensity of 1 mW cm^{-2} was used as a UV light source. The wavelength range and main wavelength of light were 350–450 nm and 365 nm, respectively. The changes in the characteristic peaks of stearic acid were observed by FT-IR. The changes in methyl orange concentration were determined tracking changes in transmission at 464 nm.

To evaluate the stability of the samples in acidic or alkaline solution, the $SiO_2/Bi_2O_3/TiO_2$ thin films were immersed in 5% wt H_2SO_4 or NaOH solution at room temperature for 24 h, followed by thorough washing with distilled water. The treated thin films were air-dried, stored in the dark at ambient conditions until subjected to water contact angle, antifogging and photocatalytic activity measurements.

3. Results and discussion

3.1. XRD analysis

The XRD patterns of prepared thin films are shown in Fig. 1. All samples exhibit a broad peak in the region of $2\theta = 15–25°$, which corresponds to amorphous SiO_2 from the glass slides. A weak diffraction peak in the region of $2\theta = 25–26°$ can be observed in Fig. 1a and c (TiO_2, T/B), suggesting that the thin films possess the anatase TiO_2 structure. For the patterns of Bi_2O_3 and B/T, the strong diffraction peak about 29° is attributed to the tetragonal structure of β-Bi_2O_3; the other peaks are ascribed to monoclinic of α-Bi_2O_3. These results show that the prepared thin films have both monoclinic and tetragonal structures, which was consistent with previous reports in the literature.[34] As expected, no TiO_2 diffraction peak was detected in B/T nor Bi_2O_3 diffraction peak detected in T/B since the bottom-layer thin films were covered by the upper films.

Fig. 1b shows the XRD the mixed thin films of Bi_2O_3–TiO_2. There is a weak diffraction peak in the region of $2\theta = 25–26°$ in all films, indicating that the addition of Bi_2O_3 did not destroy the structure of TiO_2. Fig. S1† shows the XPS spectra of Bi_2O_3–TiO_2 thin films, illustrating that they both have TiO_2 and Bi_2O_3, which was consistent with this XRD pattern result. Fig. 1d is the low angle XRD patterns, S/T exhibited a sharp diffraction peak in the region of $2\theta = 1.5–3°$, indicating that S/T retained a mesoporous structure of SiO_2 thin film, because the SiO_2 films were on the surface of S/T thin films. In contrast, in the XRD patterns of TiO_2 and Bi_2O_3 thin films in the $2\theta = 1.5–3°$ region, there are no indications of peaks, suggesting that the

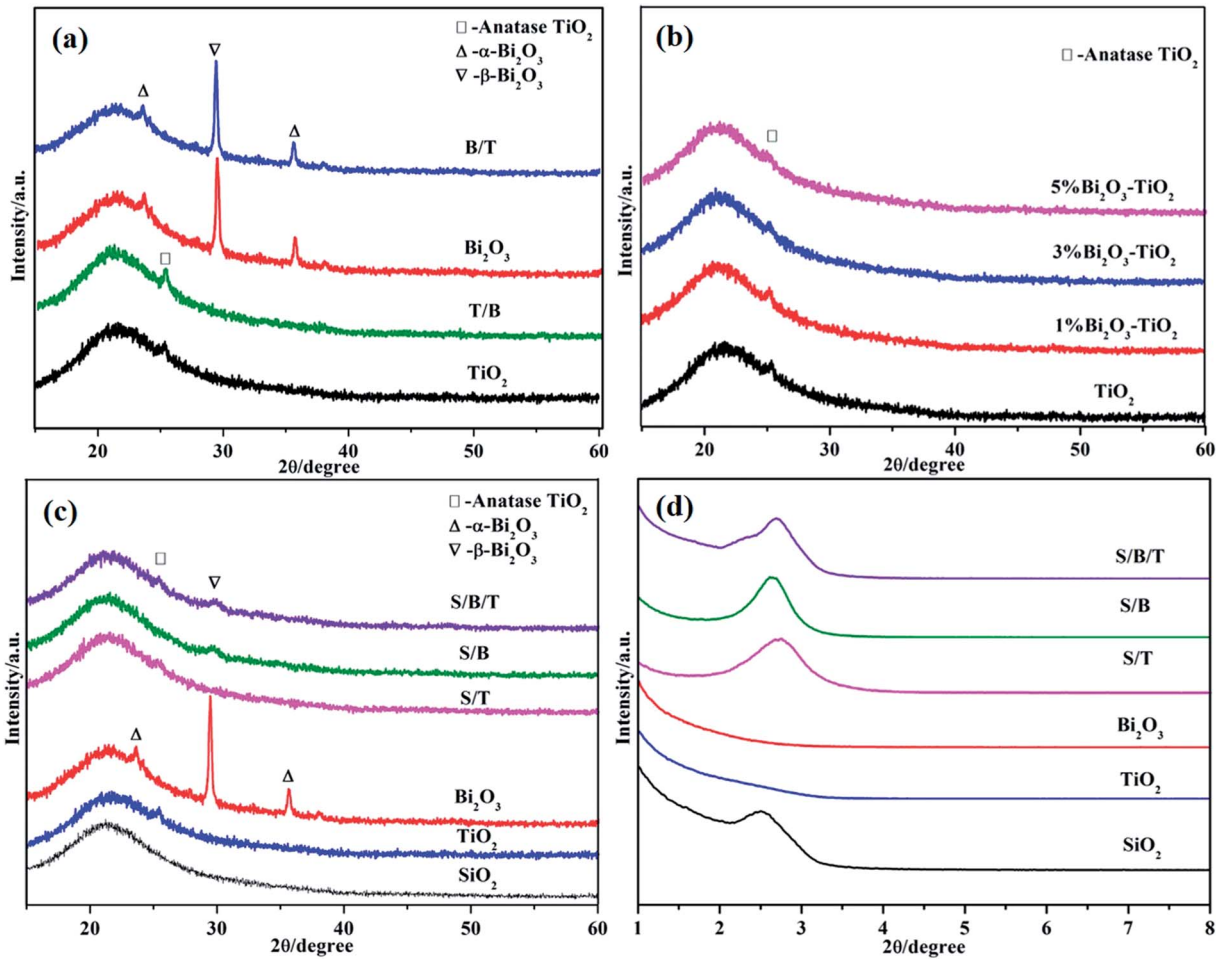

Fig. 1 XRD patterns of samples: (a) double-layered thin films, (b) mixed thin films, (c) triple-layered thin films; (d) small angle patterns of triple-layered thin films.

mesoporous structure did not exist in these two thin film surfaces. In the wide angle pattern (Fig. 1c), S/T and S/B/T show a weak diffraction peak in the region of $2\theta = 25$–26°, which is mostly ascribed to the formation of SiO_2 thin films on the surface which impeded the detection of the TiO_2.

3.2. Morphology

SEM and TEM images of the thin films surfaces are presented in Fig. 2. Nanoparticles were evenly distributed on all the thin films surfaces. However, when compared to the surface morphology of TiO_2 or Bi_2O_3, which appeared to have a smooth surface, larger nanoparticles were observed on the rough surface of T/B (Fig. S2†) and B/T. This observation can be understood as the aggregation on T/B and B/T thin films with existing Bi_2O_3 and TiO_2 nanoparticles that act as growth centers for the formation of larger nanoparticles during the calcination process, which was consistent with the XRD patterns. Fig. 2e and f show the TEM image and cross-sectional SEM image of the S/B/T thin film. TEM image shows that the S/B/T thin films possessed highly ordered mesoporous structure, which was in accordance with the presence of one-dimensional ordered hexagonal mesostructure.[35] The SEM image shows that the S/B/T thin film thickness was about 640 nm with no distinct boundary between the layers.

3.3. Optical properties

Fig. 3a and S3† show the UV-vis transmittance spectra of the films. Compared with uncoated glass (92%), all coated samples showed a decrease in transmission but still maintained a high level. S/T, S/B, and S/B/T films exhibited higher transmittance than TiO_2, Bi_2O_3 and B/T films. It is mainly due to the decrease of scattered index, which is attributed to the existence of mesoporous SiO_2 on the surface. Fig. 3b shows the visual transmission of the films. Compared with TiO_2, Bi_2O_3 and B/T, the transmittance of S/B/T was greater and displayed no visual chromatic effects. These results suggest that the introduction of SiO_2 layer can decrease the reflection of light.

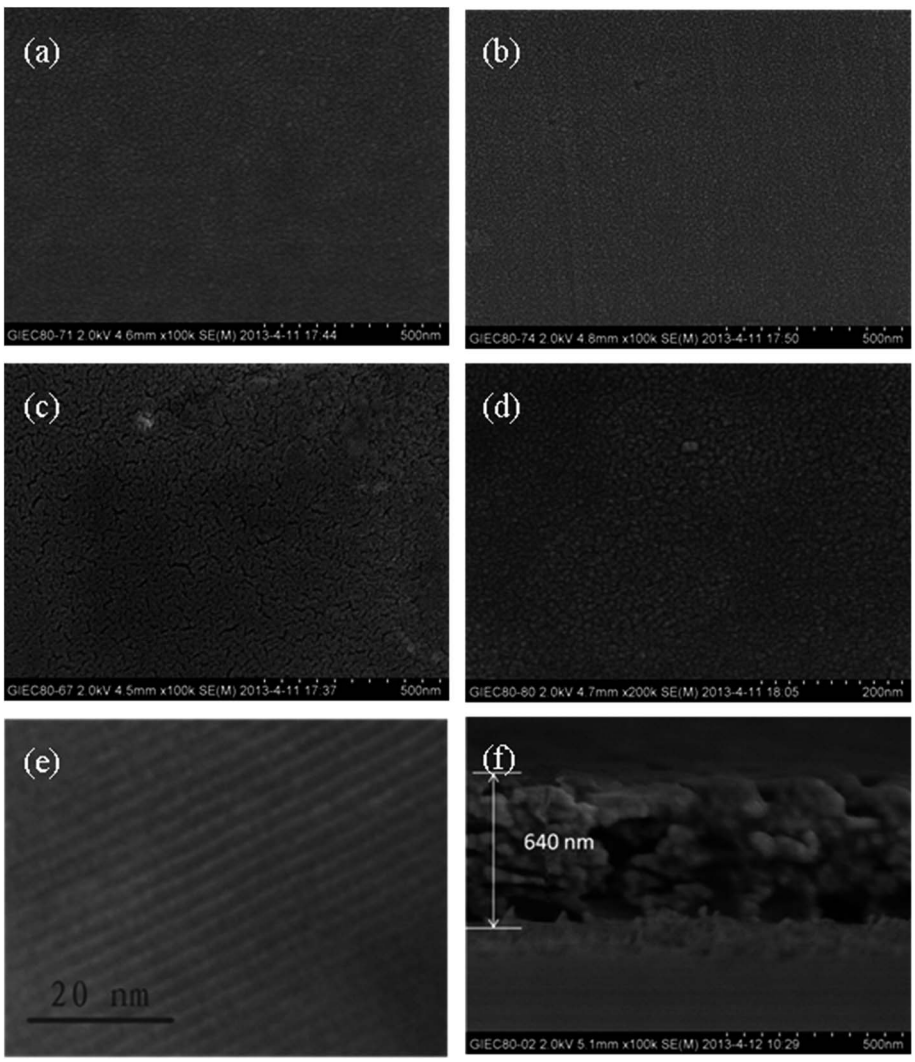

Fig. 2 SEM images of (a) TiO_2 thin film, (b) Bi_2O_3 thin film, (c) B/T thin film, (d) B–T thin film; TEM image of (e) S/B/T thin film; cross-sectional SEM image of (f) S/B/T thin film.

3.4. Superhydrophilicity and antifogging property

Fig. 4a shows the water contact angles of prepared samples when examined in the dark. The water contact angles of Bi_2O_3 and TiO_2 thin films are 118° and 29°, respectively, which confirmed that single thin films do not exhibit superhydrophilicity under dark conditions. As shown in Fig. S4,† the thin films without a mesoporous SiO_2 layer also do not possess superhydrophilicity under dark conditions. However, Fig. S5† shows that under UV irradiation the water contact angles of thin films without a SiO_2 layer became smaller, reaching a level less than 5°, which is attributed to the generation of surface hydroxide radicals. When the UV irradiation was turned off, the contact angles increased and the superhydrophilicity was lost as a result of the replacement of chemisorbed hydroxyl groups by air oxygen.[36] Fig. S5† also shows that B/T, T/B and B–T reached to superhydrophilicity state under UV light sooner than either Bi_2O_3 or TiO_2 by itself, which is evidence of the more effective separation of photo-generated electrons and holes in the composite films. Perhaps a more surprising result in Fig. 4a is the observation that the water contact angles of S/T, S/B and S/B/T thin films that possess a mesoporous SiO_2 surface layer became 0° more rapidly even under dark condition. These data show that these layered thin films exhibit superhydrophilicity even without the photoactivity associated with UV light. According to the early theoretical work by Bico and Quere *et al.*, the void fraction and surface roughness would significantly affect the wettability of a surface with water.[37,38] Our previous studies proved that a high level of wettability of SiO_2 with the mesoporous nature establishes ideal conditions for extreme wetting behaviors.[33] Therefore, the superhydrophilicity of S/T, S/B and S/B/T may be due to the increases in the number of void and pore or in the surface roughness, and all the increases would lead to a larger contact area between the water droplet and the surface coated mesoporous SiO_2, thus improving the hydrophilicity of the films.[39,40]

The antifogging behavior of these samples was explored by placing them in a freezer at −18 °C for 24 h, withdrawing them into humid air at ambient conditions and examining them for the presence of condensation (fog). Results are shown in the photographs in Fig. 4b. Fog was clearly present on the uncoated glass slide and the B/T thin film, but the glass slide

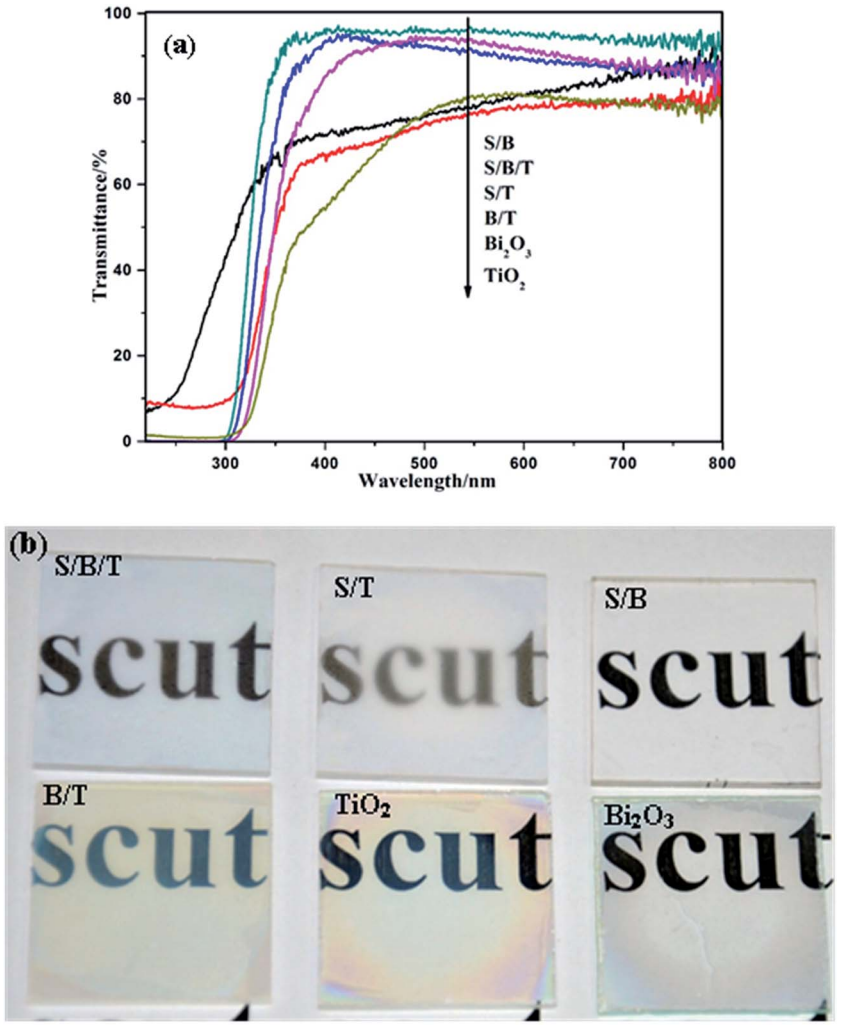

Fig. 3 (a) UV-vis transmittance spectra of the thin films; (b) photographs of the thin films.

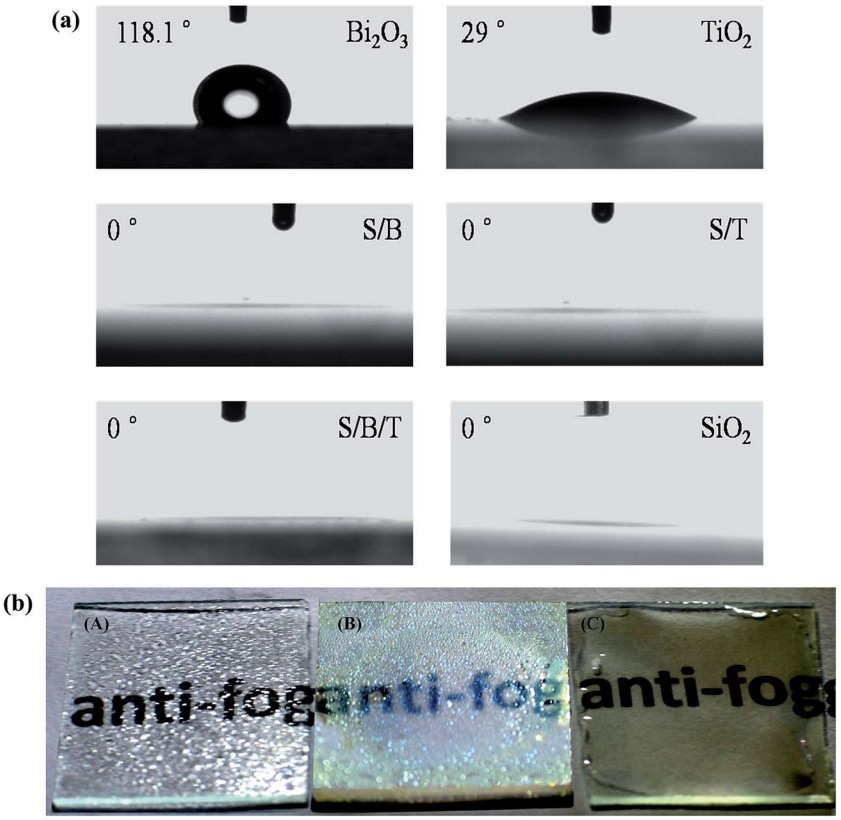

Fig. 4 (a) The images of contact angles of a water droplet on thin films in the dark; (b) fogging behavior of (A) an uncoated glass slide, (B) a glass coated with B/T thin film, (C) a glass slide coated with S/B/T thin film.

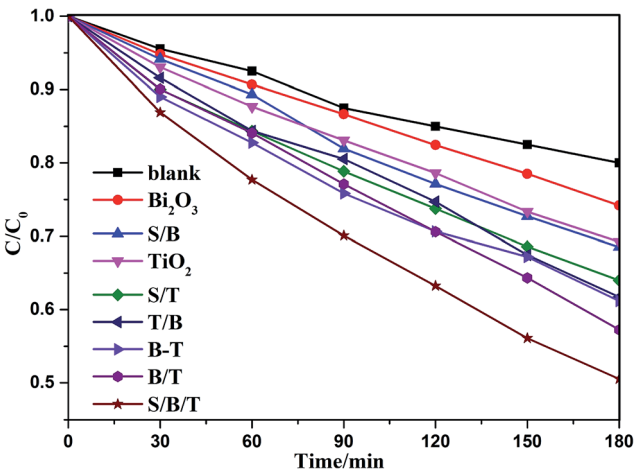

Fig. 5 Photocatalytic activity of thin films for degradation of methyl orange under UV irradiation.

coated with S/B/T still retained favorable transparency, which was due to the superhydrophilicity of the mesoporous SiO_2 thin film. These results show that the addition of the mesoporous SiO_2 layer on the surface of thin films can increase their hydrophilicity to the point of making them superhydrophilicy even in the absence of light, which is significant for self-cleaning materials.[36]

3.5. Photocatalytic property of the thin films

Photocatalytic degradation of methyl orange was carried out to determine the photocatalytic properties of the prepared thin films that, as shown in Table S1† are influenced by the number of coating layers, with the photocatalytic efficiency increasing and then decreasing with the increasing number of layers. The B(3)/T(3) film showed the highest activity, which can be understood as follows: the porosity and roughness of the membrane increased with the addition of more layers, which resulted in an increase in the specific surface area of the film, allowing for enhanced of photodegradation. As the number of layers increased further, the membrane became excessively dense, resulting in the decrease of porosity and specific surface area of the film. As a result, the photocatalytic efficiency of the thin film decreased if the film thickness increased beyond a certain point. The photocatalytic efficiencies of the Bi_2O_3–TiO_2 mixed films with different bismuth contents are shown in Fig. S6.† The concentration of methyl orange decreased with increasing time of UV illumination. The 3% B–T mixed thin film exhibited the highest activity. The addition of Bi_2O_3 could improve the separation efficiency of photo-generated charges, resulting in an enhancement of photocatalytic activity. Increasing the doping of Bi_2O_3 further led to the formation of new recombination centers for photo-generated electrons and holes, resulting in a decrease in the photocatalytic efficiency. The B/T layered films performed better than the B–T mixed film,

which is attributed to the different layer locations of Bi_2O_3 and TiO_2 in the B/T films.

Fig. 5 shows the photodegradation efficiency for methyl orange on the different thin films, with and without the surface mesoporous SiO_2 layer. The removal rates of methyl orange on S/B/T, B/T, TiO_2 and Bi_2O_3 samples were 50.10%, 42.75%, 30.75% and 25.80%, respectively. S/B/T exhibited the highest photocatalytic activity, which was improved 17.19%, 62.93% and 94.19%, respectively, compared with B/T, TiO_2 and Bi_2O_3. The result indicated that the activity of the films with mesoporous SiO_2 layer was higher than those of the films without the SiO_2 layer. According to the literature reports,[41–43] the addition of SiO_2 can be explained by providing a higher specific surface and increasing the surface hydrophilicity, which can promote the adsorption of methyl orange and increase the number of hydroxyl content in the films, with the consequence that hydrophilicity and photocatalytic activity are increased during UV irradiation thus enhances the self-cleaning effect. From the results of the present work, it can be seen that the mesoporous structure of SiO_2 has some advantages below on improvement of the photocatalytic activity. (1) It enhanced the superhydrophilicity of the films, which was beneficial for the adsorption of water and the generation of hydroxyl radical under UV irradiation. (2) It resulted in a high specific surface, which enhanced the adsorption of the solution onto the films. (3) It reduced the reflection of light and thereby increased the availability of the light to induce photodegradation. These results indicate that the mesoporous SiO_2 layer not only improved the superhydrophilicity of the films in the dark but also enhanced the photocatalytic activity of the films.

3.6. Self-cleaning of the thin film

Fig. 6a shows the photographs of water droplets on the S/B, S/T and S/B/T films after coating with stearic acid. These films have lost their superhydrophilicity, with the water contact angle moving to 52.6°, 54.6° and 55.6°, respectively. This behavior is likely a result of the formation of hydroxyl groups and the fact that the films were covered by the hydrophobic stearic acid. Nevertheless, the films recovered the superhydrophilicity gradually under UV light irradiation. As shown in Fig. 6b, after UV irradiation, the water contact angle of films coated with stearic acid decreased with the increase in the irradiation time. Finally, the contact angle of S/B, S/T and S/B/T thin films returned to 0° after 300, 240 and 180 min of irradiation, respectively. These data suggest that the prepared thin films could have a useful self-cleaning property in natural sunlight. In this regard, it is important to note that the S/B/T films performed with the highest efficiency when compared to S/B and S/T, FT-IR was used to confirm that the stearic acid was removed completely. Fig. 6c shows the FT-IR spectra of stearic acid on the films surface after different periods of UV light irradiation. Peaks at 2850 and 2925 cm^{-1} are the $-CH_2$ stretching vibrations characteristic of stearic acid.[44] These peaks became weaker as the UV irradiation time increased, disappearing completely after 3 h, signaling that the stearic acid was gone. These results are consistent with the water contact angle results. In summary, the results of the degradation studies of stearic acid and methyl orange show that S/B/T thin films display significant photocatalytic activity and superhydrophilicity, which suggest that those films possess significant self-cleaning and antifogging properties.

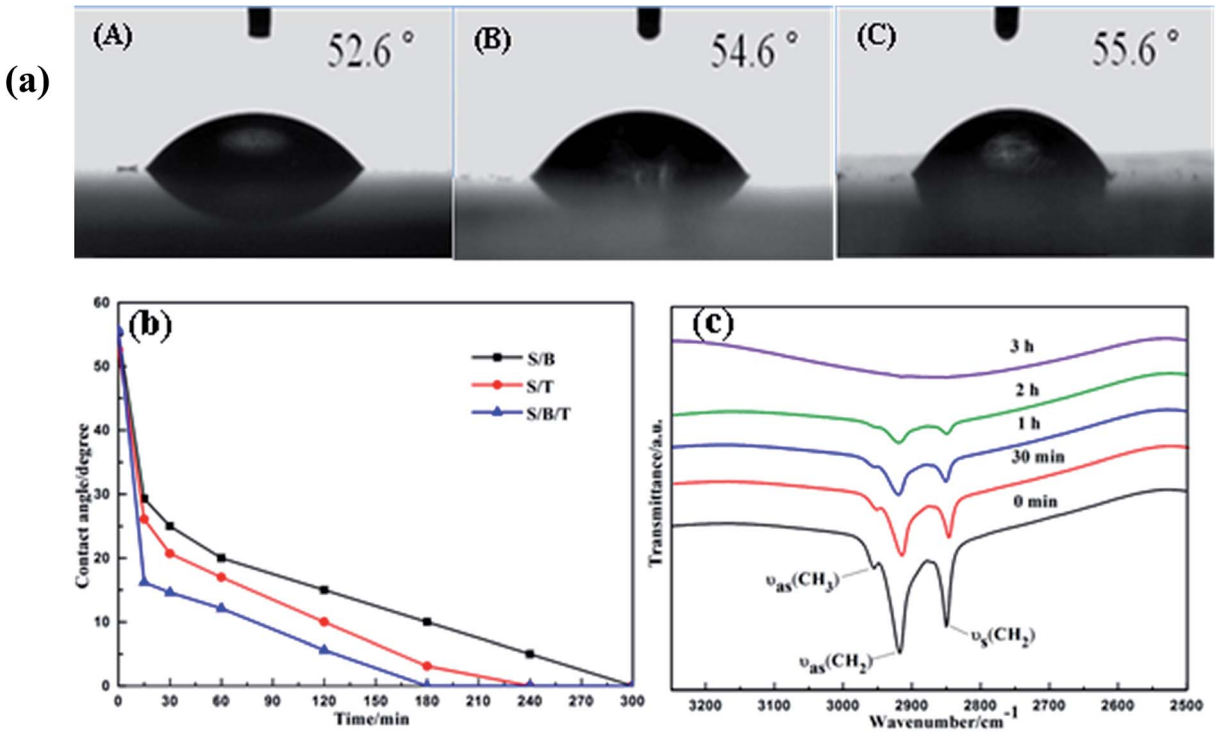

Fig. 6 (a) The images of contact angels of (A) S/T, (B) S/B, (C) S/B/T coated with stearic acid; (b) contact angle of the thin films with different irradiation times; (c) FT-IR spectra of stearic acid on the S/B/T surface with different time under UV light irradiation.

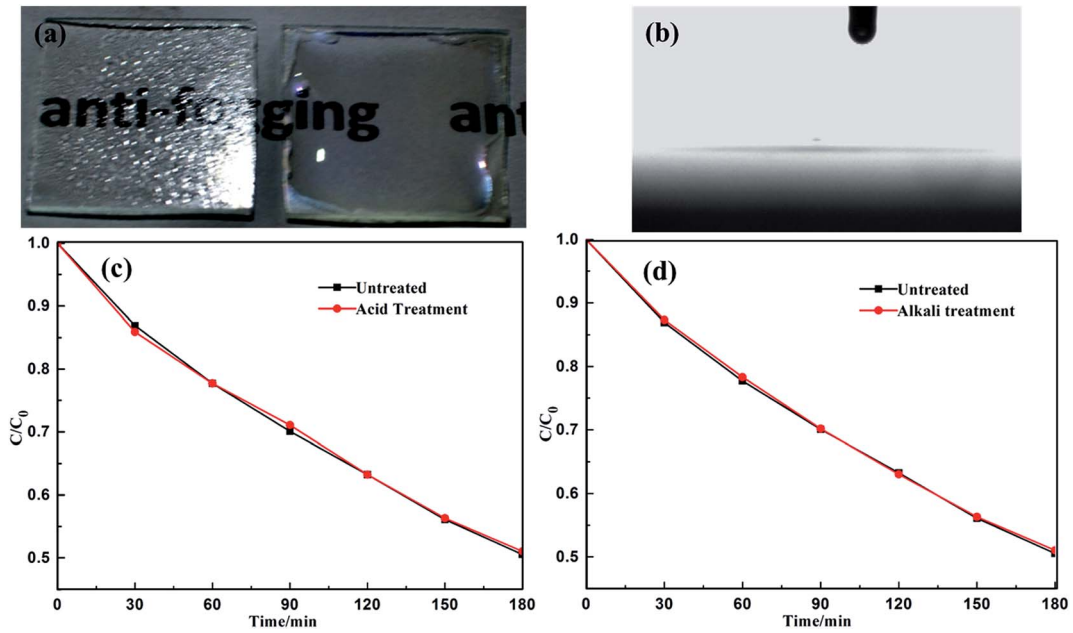

Fig. 7 Acid resistance test of the S/B/T thin film: (a) fogging behavior of uncoated glass slide (left) and S/BT thin film (right); (b) the images of contact angles of a water droplet on S/B/T thin film in the dark; (c) degradation of methyl orange after the S/B/T was treated with 5% wt H_2SO_4 for 24 h; (d) degradation of methyl orange after the S/B/T was treated with 5% wt NaOH for 24 h.

3.7. Resistance of the film to acid or alkali attack

Because of the emergence of environment pollution problems, such as acid rain, the stability of self-cleaning materials under acidic or alkaline condition is an important consideration. Therefore, the S/B/T films were immersed in 5% wt H_2SO_4 or 5% wt NaOH solution at room temperature for 24 h, followed by thorough washing with distilled water and air-drying. Fig. 7a and b are photographs of antifogging test and water contact angle of the S/B/T thin film after immersion in 5 wt% H_2SO_4 solution for 24 h. The results show that the superhydrophilicity and antifogging properties of the S/B/T film were not significantly affected by the acidic solution. Moreover, the photocatalytic activities of the films were unimpaired after the H_2SO_4 or NaOH treatment (Fig. 7c and d), indicating that the S/B/T film is stable under acidic or alkaline exposure.

4. Conclusions

Mesoporous $SiO_2/Bi_2O_3/TiO_2$ triple-layered thin films were prepared using a simple sol–gel/spin-coating method. These films possessed high transmittance and an ordered mesoporous structure that reduced the light reflection and increased the transmittance. The thin films possessed superhydrophilicity even in absence of light, as well as a significant antifogging ability. The study of the degradation of methyl orange and stearic acid demonstrated that the photocatalytic efficiency of mesoporous $SiO_2/Bi_2O_3/TiO_2$ thin films was higher than that of Bi_2O_3/TiO_2 thin films, owing to the increased light utilization and greater adsorption of pollutants in the presence of the mesoporous surface. The mesoporous $SiO_2/Bi_2O_3/TiO_2$ thin films were resistant to acidic or alkaline exposure which projects its ruggedness under today's environmental conditions. Based upon the superhydrophilicity and photocatalytic activity, mesoporous $SiO_2/Bi_2O_3/TiO_2$ thin films hold promise for use as antifogging films in the dark or on rainy days which can be a self-cleaning material when exposed to weak UV light irradiation. Therefore, self-cleaning materials possess potential value in the application for environmental pollutants control and development of new cleaning methods.

Acknowledgements

This work was supported by National Natural Science Foundation of China (21277051, 21577039), Science and Technology Planning Project of Guangdong Province, China (2015A020215004), and the Fundamental Research Funds for the Central Universities, SCUT (2015ZQ08, 2015KXKYJ07). We are grateful to Dr Donald G. Barnes for providing helpful advice to improve our paper.

References

1 X. B. Chen and S. S. Mao, *Chem. Rev.*, 2007, **107**, 2891–2959.
2 R. Wang, K. Hashimoto, A. Fujishima, M. Chikuni, E. Kojima, A. Kitamura, M. Shimohigoshi and T. Watanabe, *Nature*, 1997, **388**, 431–432.
3 Z. M. He, G. H. Guai, J. Liu, C. X. Guo, J. S. C. Loo, C. M. Li and T. T. Y. Tan, *Nanoscale*, 2011, **3**, 4613–4616.
4 X. J. Feng, J. Zhai and L. Jiang, *Angew. Chem., Int. Ed.*, 2005, **44**, 5115–5118.
5 T. Kawahara, Y. Konishi, H. Tada, N. Tohge, J. Nishii and S. Ito, *Angew. Chem., Int. Ed.*, 2002, **41**, 2811.

6 A. M. Alotaibi, S. Sathasivam and L. P. Parkin, *RSC Adv.*, 2015, **5**, 67944–67950.
7 X. Song, Y. Hu, M. M. Zheng and C. H. Wei, *Appl. Catal., B*, 2016, **182**, 587–597.
8 B. C. Weng, F. H. Xu and J. G. Xu, *RSC Adv.*, 2014, **4**, 56682–56689.
9 B. Gao, Y. J. Kim, A. K. Chakraborty and W. I. Lee, *Appl. Catal., B*, 2008, **83**, 202–207.
10 F. Tricot, F. Vocanson, D. Chaussy, D. Beneventi, M. Party and N. Destouches, *RSC Adv.*, 2015, **5**, 84560–84564.
11 X. Li, P. W. Liu, Y. Mao, M. Y. Xing and J. L. Zhang, *Appl. Catal., B*, 2015, **164**, 352–359.
12 G. Liu, L. Z. Wang, C. H. Sun, X. X. Yan, X. W. Wang, Z. G. Chen, S. C. Smith, H. M. Cheng and G. Q. Lu, *Chem. Mater.*, 2009, **21**, 1266–1274.
13 D. Li, H. Haneda, S. Hishita and N. Ohashi, *Chem. Mater.*, 2005, **17**, 2596–2602.
14 J. H. Xu, J. X. Li, W. L. Dai, Y. Cao, H. X. Li and K. N. Fan, *Appl. Catal., B*, 2008, **79**, 72–80.
15 G. Liu, Y. N. Zhao, C. H. Sun, F. Li, G. Q. Lu and H. M. Cheng, *Angew. Chem., Int. Ed.*, 2008, **47**, 4516–4520.
16 Q. C. Ling, J. Z. Sun and Q. Y. Zhou, *Appl. Surf. Sci.*, 2008, **254**, 3236–3241.
17 M. Stylidi, D. I. Kondarides and X. E. Verykios, *Appl. Catal., B*, 2004, **47**, 189–201.
18 S. Kim and W. Choi, *J. Phys. Chem. B*, 2005, **109**, 5143–5149.
19 N. Wang, L. H. Zhu, Y. P. Huang, Y. B. She, Y. M. Yu and H. Q. Tang, *J. Catal.*, 2009, **266**, 199–206.
20 C. Minero, G. Mariella, V. Maurino, D. Vione and E. Pelizzetti, *Langmuir*, 2000, **16**, 8964–8972.
21 C. Minero, G. Mariella, V. Maurino and E. Pelizzetti, *Langmuir*, 2000, **16**, 2632–2641.
22 M. Jebb, P. K. Sudeep, P. Pramod, K. G. Thomas and P. V. Kamat, *J. Phys. Chem. B*, 2007, **111**, 6839–6844.
23 C. Ratanatawanate, Y. Tao and K. J. Balkus Jr, *J. Phys. Chem. C*, 2009, **113**, 10755–10760.
24 M. H. Bartl, S. P. Puls, J. Tang, H. C. Lichtenegger and G. D. Stucky, *Angew. Chem., Int. Ed.*, 2004, **43**, 3037–3040.
25 J. S. Jang, W. Li, S. H. Oh and J. S. Lee, *Chem. Phys. Lett.*, 2006, **425**, 278–282.
26 D. Wang, X. Y. Pan, G. T. Wang and Z. G. Yi, *RSC Adv.*, 2015, **5**, 22038–22043.
27 B. J. Ma, J. S. Kim, T. Wang, J. Li, K. Y. Lin, W. Y. Liu and S. Woo, *RSC Adv.*, 2015, **5**, 79815–79819.
28 D. Chen, H. Zhang, S. Hu and J. H. Li, *J. Phys. Chem. C*, 2008, **112**, 117–122.
29 L. S. Zhang, W. Z. Wang, J. Yang, Z. G. Chen, W. Q. Zhang, L. Zhou and S. W. Liu, *Appl. Catal., A*, 2006, **308**, 105–110.
30 L. G. Wang, J. Y. Zhang, C. Z. Li, H. L. Zhu, W. W. Wang and T. M. Wang, *J. Mater. Sci. Technol.*, 2011, **27**, 59–63.
31 J. J. Xu, Y. H. Ao, D. G. Fu and C. W. Yuan, *Appl. Surf. Sci.*, 2008, **255**, 2365–2369.
32 X. T. Zhang, O. Sato, M. Taguchi, Y. Einaga, T. Murakami and A. Fujishima, *Chem. Mater.*, 2005, **17**, 696–700.
33 P. Y. Chen, Y. Hu and C. H. Wei, *Appl. Surf. Sci.*, 2012, **258**, 4334–4338.
34 W. D. He, W. Qin, X. H. Wu and H. L. Ning, *Mater. Lett.*, 2007, **61**, 4100–4102.
35 N. Nishiyama, S. Tanaka, Y. Egashira, Y. Oku and K. Ueyama, *Chem. Mater.*, 2002, **14**, 4229–4234.
36 W. J. Shan, Y. Hu, M. M. Zheng and C. H. Wei, *Dalton Trans.*, 2015, **44**, 7428–7436.
37 J. Bico, C. Marzolin and D. Quere, *Europhys. Lett.*, 1999, **47**, 743–744.
38 J. Bico, U. Thiele and D. Quere, *Colloids Surf., A*, 2002, **206**, 41–46.
39 Y. Li, T. Sasaki, Y. Shimizu and N. Koshizaki, *Small*, 2008, **4**, 2286–2291.
40 Y. Li, W. Cai, B. Cao, G. Duan, F. Sun, C. Li and L. Jia, *Nanotechnology*, 2006, **17**, 238–243.
41 K. Guan, *Surf. Coat. Technol.*, 2005, **191**, 155–160.
42 C. Anderson and A. J. Bard, *J. Phys. Chem. B*, 1997, **101**, 2611–2616.
43 E. Pakdel and W. A. Daound, *J. Colloid Interface Sci.*, 2013, **401**, 1–7.
44 Q. C. Xu, D. V. Wellia, R. Amal, D. W. Liao, S. C. J. Loo and T. T. Y. Tan, *Nanoscale*, 2010, **2**, 1122–1127.

